

RSC Advances



This is an *Accepted Manuscript*, which has been through the Royal Society of Chemistry peer review process and has been accepted for publication.

Accepted Manuscripts are published online shortly after acceptance, before technical editing, formatting and proof reading. Using this free service, authors can make their results available to the community, in citable form, before we publish the edited article. This *Accepted Manuscript* will be replaced by the edited, formatted and paginated article as soon as this is available.

You can find more information about *Accepted Manuscripts* in the [Information for Authors](#).

Please note that technical editing may introduce minor changes to the text and/or graphics, which may alter content. The journal's standard [Terms & Conditions](#) and the [Ethical guidelines](#) still apply. In no event shall the Royal Society of Chemistry be held responsible for any errors or omissions in this *Accepted Manuscript* or any consequences arising from the use of any information it contains.



ARTICLE

Using a peptide segment to covalently conjugate Doxorubicin and Taxol for the study of drug combination effect†

Ya Ling,^a Yuan Gao,^b Chang Shu,^a Ying Zhou,^a Wenyong Zhong^{*ac} and Bing Xu^d

Received 00th January 20xx,
Accepted 00th January 20xx

DOI: 10.1039/x0xx00000x

www.rsc.org/

Doxorubicin (Dox) and Taxol can be covalently bonded to the same peptide segment via proper structural modification. Doxorubicin-maleimide derivative links to peptide via Michael addition reaction and Taxol-Succi-NHS active ester connects to the same peptide backbone through ester-amide exchange reaction. Enzymatic transformation, as an inherent biological process, is applied here to trigger the formation of nanofiber networks from the as prepared hydrogelator precursor. The precursor which loads equal molar ratio of Dox and Taxol can self-assemble to form a red stable hydrogel after dephosphorylation reaction catalyzed by alkaline phosphatase (ALP). This hydrogel could maintain sustained release of drugs and show strong anticancer effect. This work, as a new strategy to build a co-delivery system of covalently linked Dox and Taxol, owns the potential to serve as an injectable hydrogel for therapeutic applications.

Introduction

Combination effect describes the phenomenon that two or more drugs act together and yield a total effect greater than the single drug efficacy.^{1,2} Drug combination has been demonstrated as an effective therapy,³ and even routinely used to treat disease such as AIDS,^{4,5} diabetes,⁶ and cancer.⁷ In practical therapy, it is capable to adjust dosages to achieve the desired ratio among chemotherapeutic agents at administration step, but it remains challenging to control the ratio between drugs which are simply mixed for administration.⁸ Doxorubicin (Dox)⁹ and Taxol¹⁰ as effective antineoplastic agent are widely used in chemotherapy.

Dox can combine with DNA to prevent further DNA and RNA biosynthesis¹¹ while Taxol can stabilize microtubule which leads to the inhibition of cell division and proliferation.¹² It has been reported that the combination of Dox and Taxol is the first-line therapeutic method of metastatic breast cancer.^{13, 14} Recent researches aiming at the co-delivery of Dox and Taxol have involved a range of systems based on polymers, including polymeric hydrogel,¹⁵ nanoparticles^{16, 17} etc. However, it is hardly to control the drug loading process precisely, as well as the enhancement of the anti-tumor efficacy.¹⁸ Certain synthetic Peptides, in most case serving as nontoxic carriers with good biodegradability and biocompatibility, can self-assemble to form hydrogels.¹⁹ It is achievable to realize the controlled and quantitative release of single drug when covalently conjugated to suitable peptide carriers.²⁰ In principle, it is feasible to release multiple drugs (e.g., Dox and Taxol) and manipulate release ratio as desired between cargos to maximize the combination effect. Here, we establish a drug delivery model which can release those two drugs at a fixed ratio of 1:1.

In previous study, it has been illustrated that NapFF^{21, 22} is a perfect motif for converting bioactive molecular into hydrogelators. Moreover, it can also enable other biofunctional molecules to self-assemble into nanostructures.²³ As proved by some clinical drugs

^a Department of analytical chemistry, China Pharmaceutical University, Nanjing, China

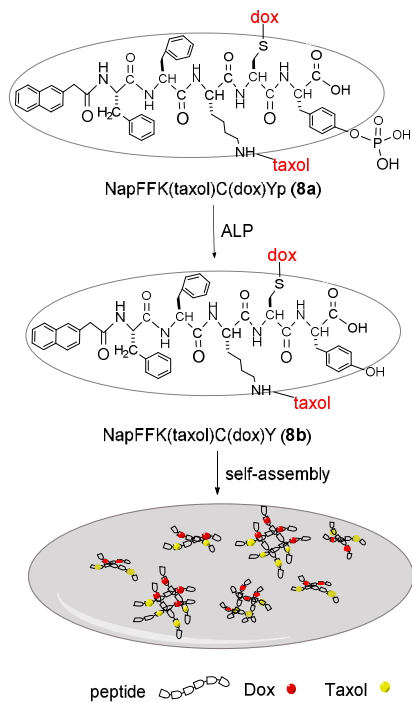
^b CAS Key Lab for Biological Effects of Nanomaterials and Nanosafety, National Center for NanoScience and Technology, 11 Beiyitia, ZhongGuanCun, Beijing 100190 (China)

^c Key Laboratory of Biomedical Functional Materials, China Pharmaceutical University, Nanjing 210009, PR China. E-mail: wyzhong@cpu.edu.cn

^d Department of Chemistry, Brandeis University, 415 South St., Waltham, MA 02454, USA

† Electronic Supplementary Information (ESI) available: The synthetic route of peptide NapFFKCYp, ¹H NMR, ³¹P NMR and MS spectra of NapFFKCYp; the synthetic route of MA-Gly-NHS, ¹H NMR spectra of GMA, GMI, MA-Gly-NHS and MS spectrum of MA-Gly-NHS; the synthetic route of Dox-Gly-MA, ¹H NMR and MS spectra of Dox-Gly-MA; the synthetic route of Taxol-Succi-NHS, ¹H NMR and MS spectra of Taxol-Succi-NHS; the synthetic route of NapFFKC(dox)Yp, ¹H NMR and MS spectra of NapFFKC(dox)Yp; the synthetic route of NapFFK(taxol)C(dox)Yp, ¹H NMR and MS spectra of NapFFK(taxol)C(dox)Yp; the TEM images of 8b at different time; the separation profile of Dox and Taxol in HPLC; the ³¹P NMR spectra of 8a and 8b. See DOI: 10.1039/x0xx00000x

(such as Naphazoline) consisted of a naphthalene (Nap) motif, Nap is more biocompatible than N-(fluorenyl-methoxycarbonyl) (Fmoc).²⁴ Aromatic-aromatic interactions and hydrogen bonds not only stabilize the structure of proteins^{25, 26} but also play an important role during the self-assembly of hydrogelators.^{27, 28} We have successfully connected Taxol (via succinic acid) to ϵ -NH₂ on the side chain of lysine in a self-assembly motif and obtained a Taxol containing hydrogel for drug release.²¹ To retain the known molecular structure maximally and facilitate the synthesis, we adopt another ligation reaction orthogonal to the amide bond formation. Here in our rational design, we chose Michael addition to append Dox molecule to a self-assembly motif. Bearing the molecular structure design in mind, we can obtain the desired Dox and Taxol conjugate by connecting NapFFKCYp (**1**), Doxorubicin-maleimide (**2**), and Taxol-succi-NHS (**3**) in order. As illustrated in Scheme 1, we designed the co-delivery system of drugs that consisted of (1) NapFFKCYp as the motif of hydrogelator, (2) Doxorubicin and Taxol as anticancer drugs which are covalently attached to the peptide for the treatment effect. (3) Self-assembly of peptide into nanofibers by dephosphorylation of alkaline phosphatase (ALP) plays the roles of a combination administration in drug delivery system.^{29, 30}



Scheme 1 The formation mechanism of the Dox-peptide-Taxol hydrogel.

Results and discussion

Formation of hydrogel

We connected Dox-Gly-MA (**2**) to the sulfhydryl group of Cysteine according to the Micheal addition reaction and Taxol-Succi-NHS active ester (**3**) to the amino of Lysine based on ester-amide exchange reaction. As illustrated in Fig. 1, the Dox and Taxol can be covalently connected with peptide (NapFFKCYp) by structural transformation. Once the system was successfully established, self-assembly can be initiated by the treatment of ALP. Upon the addition of ALP to each precursor solution, we can get hydrogels with different structures and properties. After dissolving 2 mg of **8a** in water and adjusting the pH to 7.6 with Na₂CO₃ solution, 0.10 mL PBS solution containing ALP (38 U/mL) was added (final concentration of the **8a** is 1.0 wt%). The solution became viscous after the addition of the enzyme and turned into a red solid hydrogel (Gel_{bb}, Fig. 2B) within three hours at room temperature. As illustrated in Fig. S16[†], ³¹P NMR spectra also confirm the dephosphorylation of the peptide which coincides with the enzyme-catalysed gelation mechanism. In addition, we added alkaline phosphatase (ALP) into precursor **1a** (Scheme S1) to evaluate the enzymatic hydrogelation of the peptide. After dissolving 2 mg of **1a** into 0.20 mL of water (pH=7.6) containing 0.10 mL ALP (38 U/mL), we got a white stable gel (Gel_{1b}, Fig. 2A) within 30 min at room temperature. All hydrogel catalyzed by ALP remained stable for at least 6 months without disturbing. These results demonstrate that the peptide NapFFKCYp (**1a**) as a good motif to hydrogelation has already converted into **1b** (Scheme S1) which is less soluble than **1a** and self-assembled to form hydrogel with good gelling property.

TEM and SEM images of the hydrogels

The transmission electron microscopy (TEM) is used to disclose the microscopic change in the macroscopic phase transition triggered by ALP. TEM image shows an ordered nanostructure (e.g. nanofibers) caused by self-assembly of hydrogelators. According to the TEM image of **8b** (Fig. 2D), the solution turns into the hydrogel after the addition of ALP, which exhibits inter-crossing nanofibers with a width of 40 nm. As shown in Fig. 2C, hydrogel formed by **1b**

exhibits longer, thinner, and more uniform nanofibers with a width of 20 nm, and it seems that smaller molecular is in favour of self-assembly. As illustrated in Fig. S17[†], the nanofibers expand outwards from the amorphous area. The TEM images at different time obviously show the growth of nanofibers, which further confirms the self-assembly of hydrogelators upon enzyme catalysis. Moreover, scanning electron micrograph (SEM) images of peptide (**1b**, Fig. 2E) and Dox-peptide-Taxol (**8b**, Fig. 2F) also show fibrous network microstructures which are in coincidence with what TEM images show.

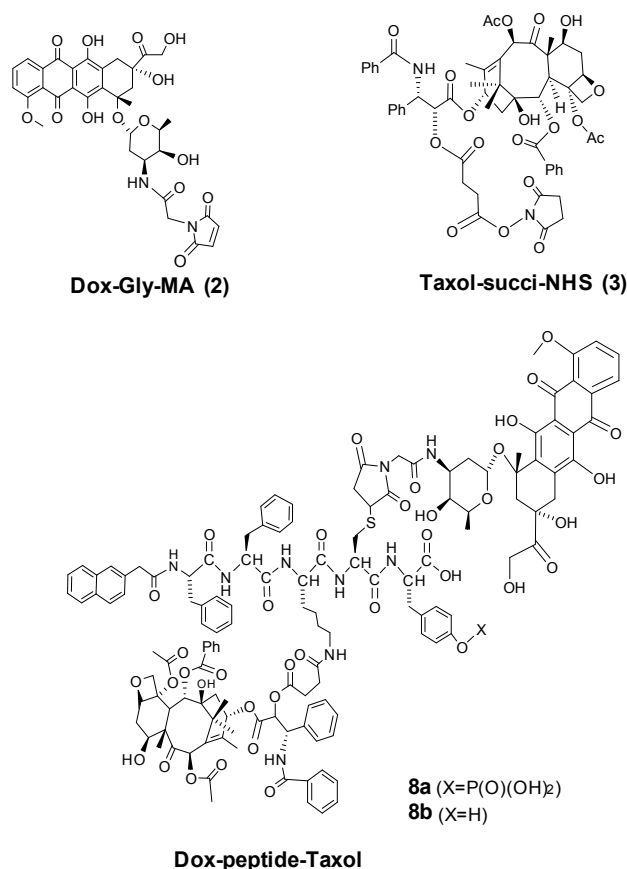


Fig. 1 The chemical structure of Doxorubicin-maleimide (**2**), Taxol-succi-NHS (**3**) and Dox-peptide-Taxol (**8a**, **8b**).

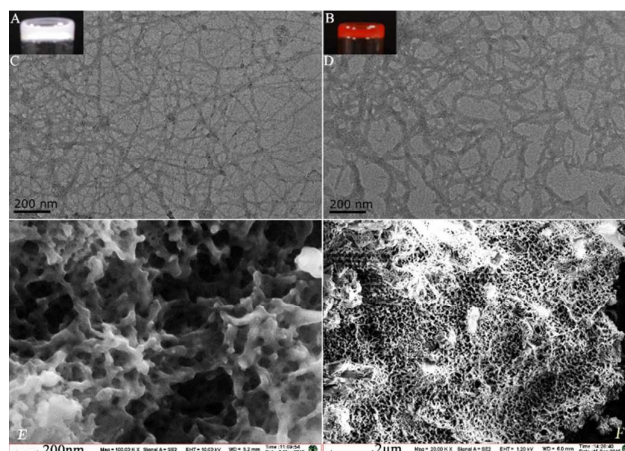


Fig. 2 Optical images of hydrogel **1b** (A) , **8b** (B) at 1.0wt%, the corresponding TEM images (C, D) at the scale of 200 nm and comparable SEM images of hydrogel **1b** (E) and hydrogel **8b** (F) .

Rheology of hydrogel

A rheological measurement is used to examine the viscoelastic properties of the hydrogel.^{31, 32} The dynamic frequency sweep under constant strain of 1% (Fig. 3A) indicates that hydrogel is slightly dependent on the frequency from 0.1 to 100 rad/s, suggesting the existence of a weak elastic matrix in hydrogel. Furthermore, their storage moduli (G') in dynamic frequency sweep are far greater than loss moduli (G''), which indicates the good viscoelasticity of hydrogel. As shown in Fig. 3B, the result of dynamic strain (0.1~10 % strain, 6.28 rad/s frequency) sweep dominates that hydrogel was destroyed once applied strain beyond critical value (6.5 %). G' and G'' obviously appear declining and G'' is higher than that of G' , which indicates the transformation of the gel to the solution. Rheology with the mode of dynamic time sweep is used to characterize the recovery of the enzymatic hydrogelation after subjected to 1000 s⁻¹ shear for 30 s. As illustrated in Fig. 3C, when the value of G' is greater than G'' , the solution of **8b** transferred into the gel, verifying its shear-thinning and recovery properties which can be used in injectable hydrogel.^{33, 34} All results suggest that Dox-peptide-Taxol is an effective hydrogel which holds good mechanical properties.

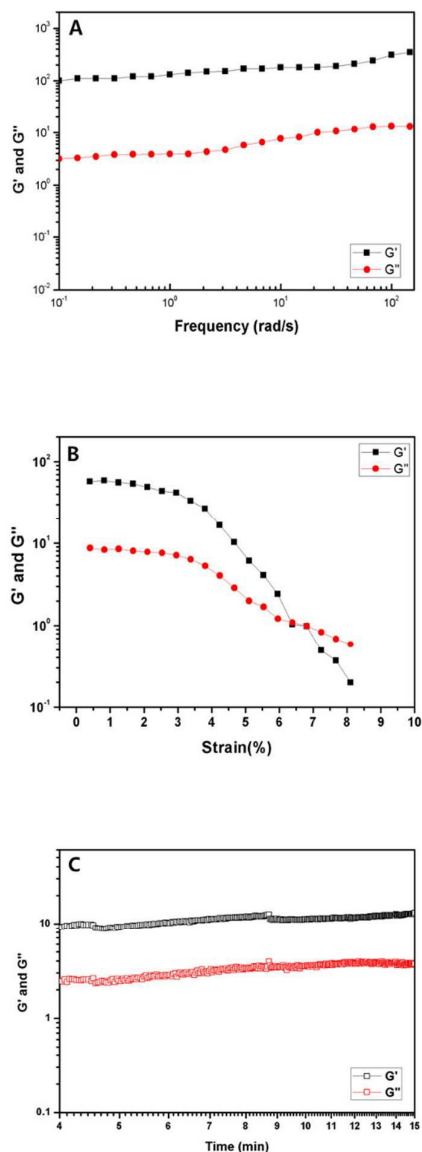


Fig. 3 (A) Dynamic frequency sweep (0.1~100 rad/s frequency, 1% strain) and (B) dynamic strain sweep (0.1~10% strain, 6.28 rad/s frequency) and (C) dynamic time sweep of 1.0% wt% Dox-peptide-Taxol hydrogel at 37 °C (6.28 rad/s frequency, 1% strain).

In vitro drugs release

The drug release is investigated in PBS solutions. Drug release from 1.0 wt% hydrogel is plotted in Fig. 4. Sustained releases of Dox and Taxol are observed in 72 hours. Dox is released at a constant rate of about 1.25 $\mu\text{g}/\text{mL}$ per hour, while the release rate for Taxol is 1.43 $\mu\text{g}/\text{mL}$ per hour. The lower release rate of Dox is due to the

hydrogen bond between peptide and Dox which limits the release of Dox from hydrogel. Both drugs exhibit similar profile and have no initial burst release. The empirical Ritger-Peppas equation was used to determine the possible mechanism of the drug release.³⁵ The value of exponential factors (n) are 0.8941 ($k=0.9945$), 0.9473 ($k=0.9969$) for Dox and Taxol respectively, n between 0.5 and 1 indicates releasing mechanism of non Fickian diffusion. This further verifies that the release of drugs from hydrogel follows the two correspond processes, one is diffusion controlled drug release and the other is chemical covalent bonding rupture.

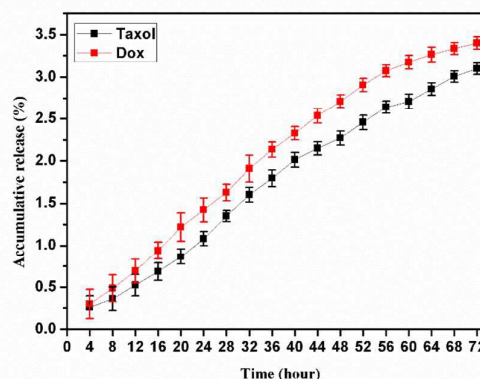


Fig. 4 Accumulative release profile of Dox and Taxol from hydrogel (1.0 wt%) at 37 °C in 0.1M PBS solution (pH 7.4, $n=3$).

Cytotoxicity

To determine the efficacy of two drugs (Dox and Taxol) after combining with peptide into hydrogelator, MTT assay was used to examine the viability of MCF-7 cells which were cultured with free peptide, peptide hydrogel, peptide-Taxol, peptide-Dox, Dox-peptide-Taxol, Dox-peptide-Taxol hydrogel, free drug of Taxol and Dox for 24 h at 37 °C. As illustrated in Fig. 5, Dox-peptide-Taxol and its hydrogel inhibited the growth of cells more strongly than peptide loaded with a single drug. The IC_{50} values of the free Taxol, Dox, Taxol-peptide and Dox-peptide are 33.79 \pm 3.12 nM, 35.56 \pm 3.62 nM, 39.84 \pm 2.03 nM, 41.39 \pm 2.16 nM respectively comparable to the IC_{50} values of dox-peptide-Taxol (18.21 \pm 1.82 nM) and Dox-peptide-Taxol hydrogel (15.62 \pm 2.42 nM). These data indicate that the modification of Taxol and Dox could retain their antitumor activity. Moreover, peptide and its hydrogel without drugs exhibit no

obvious toxicity to the cells whose IC_{50} values are more than 500 nM. All these results suggest that the peptide is a non-toxic carrier and that the anticancer effect of the drug-loaded hydrogel is significantly enhanced by co-delivery of Dox and Taxol *in vitro* assay.

Intracellular imaging

Dox itself gives a strong red fluorescence upon excitation, Thus, confocal microscopy can be used to visualize the up-take and localization of Dox-peptide-Taxol hydrogel inside the cells.³⁶ MAD-MB-231 cells were incubated with different concentrations of Dox-peptide-Taxol hydrogel while cells without drugs were used as control. After treating cells with 2.59 μ M hydrogel for 1 hour, we observed weak fluorescence inside the cell (Fig. 6-a, b, c). the cells remained almost intact. When the cells were incubated with 259 μ M hydrogel, as shown in Fig. 6-d, e, f, most of the red fluorescence was inside the cells. The intensity was significantly increased and cells became bloat and abnormal. As shown by fluorescence images of the cells incubated with 2.59 mM hydrogel (Fig. 6-g, h, i), all of the cells exhibited strong fluorescence and cells apparently began to bleb and apoptosis, indicating that the drugs have played the efficacy of anticancer. The survival time of MAD-MB-231 cells after administering high concentration hydrogel was much shorter than that of low concentration. These results agree with the fact that the co-delivery of drugs has a strong antitumor effect.

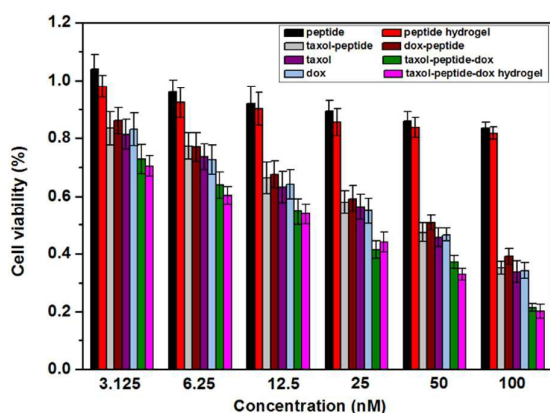


Fig. 5 Cytotoxicity of peptide, peptide hydrogel, Taxol-peptide, Dox-peptide, Taxol, Dox, Dox-peptide-Taxol, Dox-peptide-Taxol hydrogel after incubated with MCF-7 cells for 24 h.

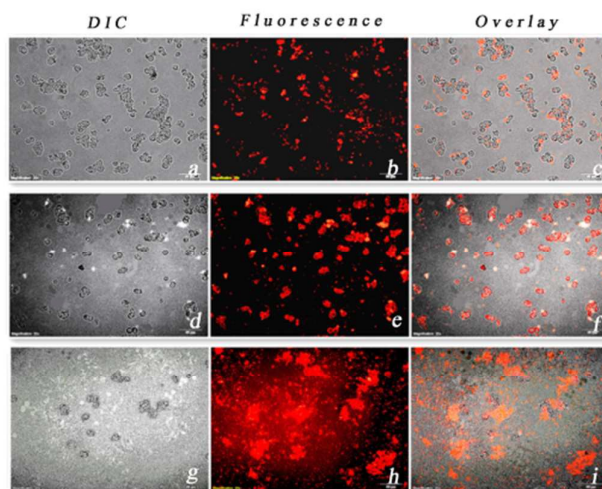


Fig. 6 Confocal images of MAD-MB-231 cells after incubation with 2.59 μ M (a, b, c), 259 μ M (d, e, f), 2.59 mM (g, h, i) Dox-peptide-Taxol hydrogel.

Conclusions

In summary, we have successfully developed a co-delivery system by covalently bonding Dox and Taxol with peptide, which exhibits improved drug efficacy. Moreover, through proper design of molecule, the combination of enzymatic reaction and self-assembly of peptide provides a facile strategy to form a supramolecular hydrogel. In our present research, we have studied the hydrogel mechanical properties, morphology, drug release *in vitro* and cytotoxicity. MTT assay and confocal microscopy images show that Dox-peptide-Taxol hydrogel not only maintains the efficacy of each drug but also display a strong joint anti-tumor effect, while peptide segment bears good biocompatibility to cells. At this point, a new delivery system that can deliver two or more drugs at controlled release ratio provides a new route for drug administration. Drug release *in vivo* and pharmacokinetic studies needs to be proved in further animal experiences.

Acknowledgements

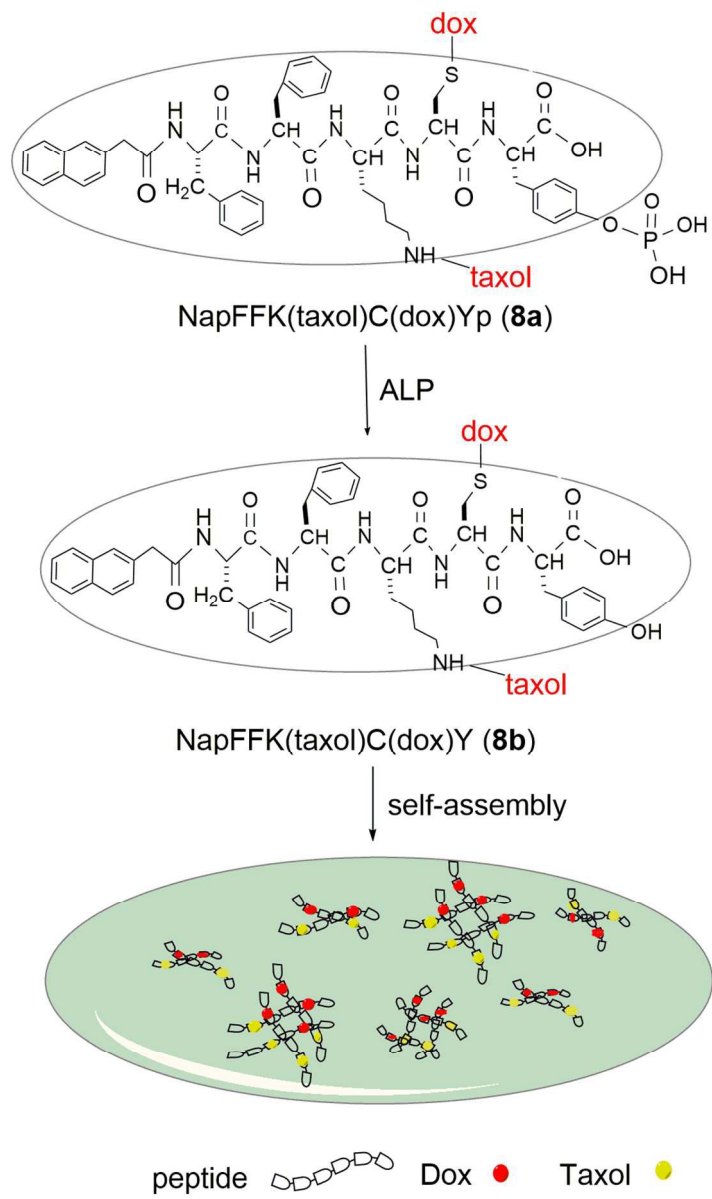
The authors gratefully acknowledge the financial support from The National Natural Science Foundation of China (No.81173023) and Priority Academic Program Development of Jiangsu Higher Education Institutions (PAPD).

Notes and references

RSC Advances

Journal Name

1. H. B. Ruttala and Y. T. Ko, *Colloids and Surfaces B: Biointerfaces*, 2015, **128**, 419-426.
2. K. Hu, H. Zhou, Y. Liu, Z. Liu, J. Liu, J. Tang, J. Li, J. Zhang, W. Sheng and Y. Zhao, *Nanoscale*, 2015, **7**, 8607-8618.
3. X. Guo, P. Wang, Q. Du, S. Han, S. Zhu, Y. Lv, G. Liu and Z. Hao, *Drug research*, 2015, **65**, 199-204.
4. S. Wildum, H. Zimmermann and P. Lischka, *Antimicrobial agents and chemotherapy*, 2015, **59**, 3140-3148.
5. S. Burgess, N. Partovi, E. M. Yoshida, S. R. Erb, V. M. Azalgara and T. Hussaini, *Annals of Pharmacotherapy*, 2015, 1060028015576180.
6. S. Bahadursingh, C. Mungalsingh, T. Seemungal and S. Teelucksingh, *Diabetology & metabolic syndrome*, 2014, **6**, 1-9.
7. S. Soukasene, D. J. Toft, T. J. Moyer, H. Lu, H. K. Lee, S. M. Standley, V. L. Cryns and S. I. Stupp, *ACS nano*, 2011, **5**, 9113-9121.
8. B. S. Wong, S. L. Yoong, A. Jagusiak, T. Panczyk, H. K. Ho, W. H. Ang and G. Pastorin, *Advanced drug delivery reviews*, 2013, **65**, 1964-2015.
9. X. Hu, W. Wei, X. Qi, H. Yu, L. Feng, J. Li, S. Wang, J. Zhang and W. Dong, *Journal of Materials Chemistry B*, 2015, **3**, 2685-2697.
10. C. Shu, R. Li, Y. Yin, D. Yin, Y. Gu, L. Ding and W. Zhong, *Chemical communications*, 2014, **50**, 15423-15426.
11. M. F. Goodman and G. M. Lee, *Journal of Biological Chemistry*, 1977, **252**, 2670-2674.
12. E. Harper, W. Dang, R. G. Lapidus and R. I. Garver, *Clinical cancer research*, 1999, **5**, 4242-4248.
13. P. Dombernowsky, J. Gehl, M. Boesgaard, T. P. Jensen, B. W. Jensen and B. Ejlersen, 1995, **22**, 13-17.
14. J. Gehl, M. Boesgaard, T. Paaske, B. V. Jensen and P. Dombernowsky, *Annals of oncology*, 1996, **7**, 687-693.
15. L. Zhao, L. Zhu, F. Liu, C. Liu, Q. Wang, C. Zhang, J. Li, J. Liu, X. Qu and Z. Yang, *International journal of pharmaceuticals*, 2011, **410**, 83-91.
16. H. Wang, Y. Zhao, Y. Wu, Y.-I. Hu, K. Nan, G. Nie and H. Chen, *Biomaterials*, 2011, **32**, 8281-8290.
17. J. Miao, Y.-Z. Du, H. Yuan, X.-g. Zhang and F.-Q. Hu, *Colloids and Surfaces B: Biointerfaces*, 2013, **110**, 74-80.
18. L. Gianni, E. Munzone, G. Capri, F. Fulfarò, E. Tarenzi, F. Villani, C. Spreafico, A. Laffranchi, A. Caraceni and C. Martini, *Journal of clinical oncology*, 1995, **13**, 2688-2699.
19. N. Stephanopoulos, J. H. Ortony and S. I. Stupp, *Acta materialia*, 2013, **61**, 912-930.
20. H. Wang, J. Wei, C. Yang, H. Zhao, D. Li, Z. Yin and Z. Yang, *Biomaterials*, 2012, **33**, 5848-5853.
21. Yuan Gao, Yi Kuang, Zu-Feng Guo, Zhihong Guo, Isaac J. Krauss and Bing Xu, *Journal of the American Chemical Society*, 2009, **731**, 13576-13577.
22. Y. Zhang, Y. Kuang, Y. Gao and B. Xu, *Langmuir : the ACS journal of surfaces and colloids*, 2011, **27**, 529-537.
23. H. M. Wang and Z. M. Yang, *Nanoscale*, 2012, **4**, 5259-5267.
24. F. Zhao, M. L. Ma and B. Xu, *Chemical Society Reviews*, 2009, **38**, 883-891.
25. E. N. G. Marsh, *Accounts of chemical research*, 2014, **47**, 2878-2886.
26. C. N. Pace, H. Fu, K. Fryar, J. Landua, S. R. Trevino, D. Schell, R. L. Thurlkill, S. Imura, J. M. Scholtz and K. Gajiwala, *Protein Science*, 2014, **23**, 652-661.
27. B. H. Jones, A. M. Martinez, J. S. Wheeler and E. D. Spörke, *Soft matter*, 2015, **11**, 3572-3580.
28. W. Jianwei, S. Lifeng, Z. Jin and Y. Xubo, *PROGRESS IN CHEMISTRY*, 2015, **27**, 373-384.
29. J. Li, Y. Gao, Y. Kuang, J. Shi, X. Du, J. Zhou, H. Wang, Z. Yang and B. Xu, *Journal of the American Chemical Society*, 2013, **135**, 9907-9914.
30. Zhimou Yang, Gaolin Liang, Ling Wang and Bing Xu, *Journal of the American Chemical Society*, 2005, **128**, 3038-3043.
31. C. Yan and D. J. Pochan, *Chemical Society Reviews*, 2010, **39**, 3528-3540.
32. A. I. Van Den Bulcke, B. Bogdanov, N. De Rooze, E. H. Schacht, M. Cornelissen and H. Berghmans, *Biomacromolecules*, 2000, **1**, 31-38.
33. A. A. Amini, H.-M. Kan, Z. Cui, P. Maye and L. S. Nair, *Tissue Engineering Part A*, 2014, **20**, 2830-2839.
34. M. R. Haque, D. Y. Lee, C.-H. Ahn, J.-H. Jeong and Y. Byun, *Pharmaceutical research*, 2014, **31**, 2453-2462.
35. L. Serra, J. Doménech and N. A. Peppas, *Biomaterials*, 2006, **27**, 5440-5451.
36. N.-T. Chen, C.-Y. Wu, C.-Y. Chung, Y. Hwu, S.-H. Cheng, C.-Y. Mou and L.-W. Lo, *PloS one*, 2012, **7**, e44947.



86x144mm (300 x 300 DPI)